OPTICS

The coherence of light is fundamentally tied to the quantum coherence of the emitting particle

Aviv Karnieli[1], Nicholas Rivera[2], Ady Arie[3], Ido Kaminer[4]*

Coherent emission of light by free charged particles is believed to be successfully captured by classical electromagnetism in all experimental settings. However, recent advances triggered fundamental questions regarding the role of the particle wave function in these processes. Here, we find that even in seemingly classical experimental regimes, light emission is fundamentally tied to the quantum coherence and correlations of the emitting particle. We use quantum electrodynamics to show how the particle's momentum uncertainty determines the optical coherence of the emitted light. We find that the temporal duration of Cherenkov radiation, envisioned for almost a century as a shock wave of light, is limited by underlying entanglement between the particle and light. Our findings enable new capabilities in electron microscopy for measuring quantum correlations of shaped electrons. Last, we propose new Cherenkov detection schemes, whereby measuring spectral photon autocorrelations can unveil the wave function structure of any charged high-energy particle.

INTRODUCTION

Excitation of waves by a moving object is ubiquitous in many areas of physics, such as electrodynamics (*1*), acoustics (*2*), and hydrodynamics (*3*)—examples are the Cherenkov effect, sound waves, and ship wakes. These processes are thought to be successfully explained by classical physics, wherein wave interference is often critical for describing the phenomena. For example, in electrodynamics (*1*), radiation emission patterns are predicted by Maxwell's equations.

Such is the case for Cherenkov radiation (CR): the emission of light by free charged particles moving faster than the phase velocity of light in a medium (*4*). Since its discovery in 1934, a long-standing hallmark of CR is its manifestation as a "shock wave" of light (*1*, *5*–*9*), resulting from the coherent temporal interference of radiation at a wide spectral range. Despite the wide applicability of this effect, no experiment has ever directly observed the shock wave dynamics emitted by a single particle. As one of the implications of this work, we shall see that the underlying quantum nature of CR fundamentally limits the shock wave duration in many existing experimental settings, which can be understood in terms of the entanglement of the light with the emitting particle.

Looking at the bigger picture in electromagnetism, light emission by free charged particles constitutes a family of effects (*10*, *11*) including, for example, transition radiation (*12*), Smith-Purcell radiation (*13*), undulator radiation (*14*), and CR. Often called coherent cathodoluminescence (*10*) (CL), these phenomena are used in many areas of physics and engineering, from electron microscopes (*10*, *15*), particle detectors (*16*, *17*), free-electron lasers (*18*), engineerable light sources (*19*, *20*), and medical imaging (*21*). As the spectral range of emitted light can be straightforwardly tuned by varying the particle energy, coherent CL is a promising platform for light generation in otherwise inaccessible regimes (*18*, *22*), such as at terahertz, ultraviolet, and x-ray frequencies.

The broad tunability of coherent CL, alongside recent advances in shaping (*23*, *24*), coherent control (*25*–*27*), and entanglement (*28*, *29*) of free electrons, makes it a probe of fundamental light-matter interaction (*15*, *30*) and a prominent candidate for quantum measurement (*15*). These advancements brought about fundamental questions regarding the role of the particle wave function (*30*–*34*) in coherent CL. However, in all relevant experimental settings, coherent CL is still considered as classical (*35*–*39*) or semiclassical (*31*, *34*, *40*, *41*). The general expectation from a quantum theory is that when the emitting particle is not directly measured (*42*), the quantum features of its wave function (*43*–*45*) cannot leave a detectable mark on the emitted light. A milestone of fundamental importance would be, therefore, to identify observables of coherent CL radiation that are both detectable in practical settings and directly depend on the quantum state of the emitting particles. This observation has implications also for general wave phenomena, such as any mechanical waves excited by free moving objects. Can fundamental quantum aspects of a particle affect the patterns of waves in seemingly classical regimes?

Here, we introduce the quantum optical paradigm to describe coherent CL and identify the specific measurements that depend on the quantum wave nature of the emitter. By formulating a general quantum theory of spontaneous light emission by charged particles, we show that already in what are generally assumed to be classical regimes, coherent CL can be dominated by quantum features such as wave function uncertainty, quantum correlations, and decoherence. These effects can be exposed in quantum optical measurements, such as first-order correlation measurements, even in seemingly classical features such as the emitted pulse duration. Although the concept of coherence transfer was thoroughly studied in quantum optics for nonrelativistic bound-electron systems [for example, in effects such as quantum beats (*46*)], it was never applied to light emission from relativistic free charged particles, still commonly described in classical or semiclassical terms. Hence, new insight is gained by analyzing the optical coherence of such system through the prism of quantum optics.

As an unexpected implication for the Cherenkov effect, we find that quantum decoherence imposes a fundamental lower bound for the Cherenkov shock wave duration, predicting an uncertainty

[1]Raymond and Beverly Sackler School of Physics and Astronomy, Tel Aviv University, Ramat Aviv, Tel Aviv 69978, Israel. [2]Department of Physics, Massachusetts Institute of Technology, Cambridge, MA 02139, USA. [3]School of Electrical Engineering, Fleischman Faculty of Engineering, Tel Aviv University, Tel Aviv 69978, Israel. [4]Department of Electrical Engineering, Technion-Israel Institute of Technology, Haifa 32000, Israel.
*Corresponding author. Email: kaminer@technion.ac.il

principle that connects it to the particle momentum uncertainty. Quantum coherence is the ability of a quantum system to demonstrate interference. The coherence between different parts of a wave function (in momentum or real space) allows for the famous double-slit interference and the formation of short quantum wave packets propagating in space. Quantum decoherence, as its name suggests, is the loss of quantum coherence, hindering the visibility of interference. Most commonly, this process happens when an open quantum system interacts with its surrounding environment (*47*). The underpinning mechanism for decoherence is the entanglement of the observed subsystem (for example, an emitted photon) with another, unobserved subsystem (for example, a charged particle). In our context, we identify many practical scenarios in which CR is not a shock wave, owing to the underlying quantum decoherence of the emitted light.

Our quantum theory of coherent CL has new applications, such as detecting the shape, size, and coherence of the emitter's wave function by measuring the spectral autocorrelations of the light it emits—thereby gaining information on the wave function uncertainty. Our findings can resolve a question, which, with the advent of ultrafast electron microscopes, has been frequently asked: What part of the measured energy spread of an electron beam is due to coherent energy uncertainty, and what part is due to incoherent uncertainty? Moreover, our work sheds light on fundamentally new capabilities to measure quantum properties of charged particles that can serve as an alternative to matter wave holography, which is especially important for many high-energy particles observed in Cherenkov detectors, where holographic techniques do not exist. The results presented in this work pave the way toward novel tunable light sources and measurements sensitive to the wave function of free charged particles.

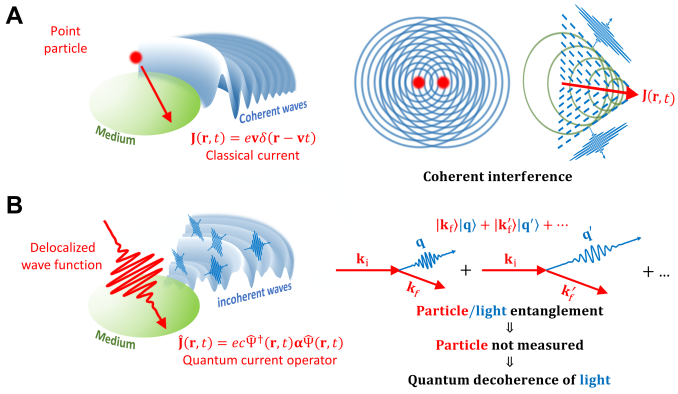

Fig. 1. Excitation of waves by free particles: classical versus quantum theory. (**A**) Classical wave dynamics. A point particle with velocity **v** passes through an optical medium and emits waves that may interfere coherently. The classical emitter current density $\mathbf{J}(\mathbf{r}, t) = e\mathbf{v}\delta(\mathbf{r} - \mathbf{v}t)$ emits a temporally coherent shock wave. (**B**) Quantum description. A quantum particle is described by a delocalized wave function $\psi(\mathbf{r}, t)$. A current operator $\hat{\mathbf{J}}(\mathbf{r}, t)$ is then associated with the particle. Even when the initial particle is only described by a single momentum $\mathbf{k}_i$, it may spontaneously emit many wave quanta (momenta $\mathbf{q}$, $\mathbf{q}'$, …). The waves are then entangled with the particle because of momentum conservation (leaving the final particle having momenta $\mathbf{k}_f$, $\mathbf{k}_f'$, … respectively). When only the emitted waves are observed, this entanglement can lead to quantum decoherence and lack of interference visibility, resulting in the emission of incoherent radiation.

RESULTS

Excitation of waves by free particles

In classical physics, waves interfere coherently when they are generated from different point particles constituting an emitter (*48*), so long as the different emission points are perfectly correlated with each other (Fig. 1A). In particular, the emission from each individual particle is considered to always be coherent with itself. In quantum mechanics, an emitter is described by a spatially varying wave function. Following the emission of wave quanta, the particles and waves are in an entangled state, known to cause quantum decoherence (Fig. 1B) (*47*) if one of the constituents of the bipartite system is not measured. As spontaneous emission of light by free charged particles is usually described classically (*35*–*39*), it is generally assumed that the abovementioned effect is negligible, on the grounds that the correspondence principle (*49*) is always valid. This assumption is backed by the small quantum recoil (*10*) exerted by the photon, amounting to only minor corrections (*43*–*45*). It is the purpose of the following analysis to show that under certain common conditions, quantum mechanics fundamentally modifies light emission, even in regimes that are traditionally seen as classical.

Recent works considered in depth the effect of the wave function size and shape on the spontaneously emitted radiation by free charged particles. Investigations based on semiclassical analysis (*31*, *34*, *40*, *41*) imply size- and shape-dependent effects on the emitted power spectrum, while a quantum analysis (*32*, *33*) suggested no such effects. Importantly, experiments have demonstrated wave function dependence upon postselection of a final electron state (*30*), while no such effects were observed when only the light was measured (no postselection) (*33*). The findings detailed below determine between the contradicting results, showing explicitly that without postselection, the wave function does not affect the power spectrum of spontaneous emission, while suggesting a new observable—spectral coherence—which explicitly depends on the wave function, and how the size and shape of the latter could be extracted from it. In this context, our findings can help promote the fast-growing field of free-electron quantum optics (*50*, *51*) and emphasize the effect of the electron wave function in ultrafast electron beam spectroscopy experiments (*15*).

Without loss of generality, consider the emitting charged particles to be free electrons. We also consider the emitted electromagnetic field to be in a general optical environment. The initial state is described by a density matrix $\boldsymbol{\rho}_i$, where the electrons have a reduced density matrix $\boldsymbol{\rho}_e$, and the radiation field is found in the vacuum state $|0\rangle$, such that the initial state is separable $\boldsymbol{\rho}_i = \boldsymbol{\rho}_e \otimes |0\rangle\langle 0|$. The interactions between the electrons and the electromagnetic field are governed by the Dirac Hamiltonian: $H_{\mathrm{int}} = ec\boldsymbol{\alpha} \cdot \mathbf{A}$, where e is the electron charge, c the speed of light, $\boldsymbol{\alpha}^i = \boldsymbol{\gamma}^0\boldsymbol{\gamma}^i$ are the Dirac matrices, and $\mathbf{A}$ is the electromagnetic vector potential operator. Considering a weak coupling between the electrons and photons, the final quantum state of the system, $\boldsymbol{\rho}_f$, is found by first-order time-dependent perturbation theory (see section S1).

In general, after the interaction, the electrons are entangled to many photonic modes because emission is allowed for different directions and at many different frequencies. For example, starting from an arbitrary initial wave function of a single electron and zero photons, $|\psi_i\rangle = \sum_{\mathbf{ki}} \varphi_{\mathbf{ki}} |\mathbf{k}_i\rangle |0\rangle$, and if momentum is conserved—as in CR—the photon can be emitted with different momenta $\mathbf{q} = \mathbf{k}_i - \mathbf{k}_f$, giving an entangled final state

$$|\psi_f\rangle = \sum_{\mathbf{k}_i}\varphi_{\mathbf{k}_i}\sum_{\mathbf{k}_f}M_{\mathbf{k}_i\to\mathbf{k}_f;\mathbf{q}}\,e^{-iE_f t/\hbar}e^{-i\omega_q t}\,|\mathbf{k}_f\rangle\,|\mathbf{q}=\mathbf{k}_i-\mathbf{k}_f\rangle \quad (1)$$

where $M_{\mathbf{ki}\to\mathbf{kf};\mathbf{q}}$ is the transition amplitude. Information regarding the electron initial state $\varphi_{\mathbf{ki}}$ can be extracted by measuring the photon momentum $\mathbf{q}=\mathbf{k}_i-\mathbf{k}_f$ in coincidence with (or postselection of) an electron momentum $\mathbf{k}_f$. However, this is not the experimental situation of CL, where only the light is measured, and the electron degrees of freedom are traced out. In this case, both experimental and theoretical evidence suggest that the initial electron wave function has no influence on observables of the emitted radiation (*32*, *33*, *44*), such as the power spectrum. Below, we will examine this situation carefully and show how the emitted light autocorrelations can be strongly influenced by the single electron wave function—although the power spectrum is not, suggesting a ubiquitous, hidden quantumness to the radiation by free electrons.

To describe the photonic final state in the experimental scenario of coherent CL, we calculate the reduced density matrix of the electromagnetic field, $\boldsymbol{\rho}_{ph}=\mathrm{Tr}_e\{\boldsymbol{\rho}_f\}$, with Tr_e denoting the partial trace over the electronic state. The electric field autocorrelation is determined by the final photonic state, $\boldsymbol{\rho}_{ph}$, via the quantum mechanical expectation value $\langle\mathbf{E}^{(-)}(\mathbf{r}',t')\mathbf{E}^{(+)}(\mathbf{r},t)\rangle=\mathrm{Tr}\{\mathbf{E}^{(-)}(\mathbf{r}',t')\mathbf{E}^{(+)}(\mathbf{r},t)\boldsymbol{\rho}_{ph}\}$, where $\mathbf{E}^{(+)}(\mathbf{r},t)$ and $\mathbf{E}^{(-)}(\mathbf{r},t)=(\mathbf{E}^{(+)}(\mathbf{r},t))^\dagger$ are, respectively, the positive and negative frequency parts of the electric field operator. Instead of the simplified momentum-space picture of Eq. 1, which strictly holds only for CR (see section S8), we use a more general formalism. On the basis of quantum electrodynamical perturbation theory, the formalism holds for all coherent CL processes and for an arbitrary number of electrons (see section S1 for derivation), yielding

$$\langle\mathbf{E}^\dagger(\mathbf{r}',\omega')\mathbf{E}(\mathbf{r},\omega)\rangle = \omega\omega'\mu_0^2\int d^3\mathbf{R}\,d^3\mathbf{R}'\,\mathbf{G}^\dagger(\mathbf{r}',\mathbf{R}',\omega')\mathbf{G}(\mathbf{r},\mathbf{R},\omega)\,\langle\mathbf{j}^\dagger(\mathbf{R}',\omega')\,\mathbf{j}(\mathbf{R},\omega)\rangle_e \quad (2)$$

where $\mathbf{G}(\mathbf{r},\mathbf{r}',\omega)$ is the Dyadic Green's function of Maxwell's equations for the dielectric medium (*52*), and where $\mathbf{E}^{(+)}(\mathbf{r},t)=\int_0^\infty d\omega\,e^{-i\omega t}\mathbf{E}(\mathbf{r},\omega)$. The quantity $\langle\mathbf{j}^\dagger(\mathbf{r}',\omega')\mathbf{j}(\mathbf{r},\omega)\rangle_e=\mathrm{Tr}\{\boldsymbol{\rho}_e\mathbf{j}^\dagger\mathbf{j}\}$ is the expectation value, with respect to the emitter initial state, of the correlations in the current density operator $\mathbf{j}(\mathbf{r},t)=ec\boldsymbol{\Psi}^\dagger\boldsymbol{\alpha}\boldsymbol{\Psi}$, where $\boldsymbol{\Psi}(\mathbf{r},t)$ is the emitter spinor field operator described in second quantization (see sections S1 and S2). From here onward, we assume that the particles propagate as wave packets with a well-defined carrier velocity $\mathbf{v}_0$ (the paraxial approximation, where the particle dispersion is linearized about its mean momentum/energy).

Now, let us constrain the discussion to the seemingly classical regime, where photon recoils $\hbar q$ are much smaller than electron momenta p_e. This constraint is applicable to a vast number of effects, including all cases in which the emitter is relativistic, all current free-electron nanophotonic light sources, and all free-electron sources in the microwave and radio frequency ranges. In general, this derivation applies to both the single- and many-particle emitter states, described via second quantization of the emitter. The current correlations in Eq. 2 can then be written as (see section S2 for derivation)

$$\langle\mathbf{j}(\mathbf{x}')\,\mathbf{j}(\mathbf{x})\rangle = e^2\mathbf{v}_0\mathbf{v}_0\,[\,G_e^{(2)}(\mathbf{x}',\mathbf{x})+\delta(\mathbf{x}-\mathbf{x}')\,G_e^{(1)}(\mathbf{x},\mathbf{x})\,] \quad (3)$$

where $\mathbf{x}=\mathbf{r}-\mathbf{v}_0t$ and $\mathbf{x}'=\mathbf{r}'-\mathbf{v}_0t'$. In Eq. 3, we define the first- and second-order correlation functions of the emitter $G_e^{(1)}(\mathbf{x}',\mathbf{x})=\sum_\sigma\mathrm{Tr}\{\boldsymbol{\rho}_e\,\psi_\sigma^\dagger(\mathbf{x}')\,\psi_\sigma(\mathbf{x})\}$ and $G_e^{(2)}(\mathbf{x}',\mathbf{x})=\sum_{\sigma'}\sum_\sigma\mathrm{Tr}\{\boldsymbol{\rho}_e\,\psi_{\sigma'}^\dagger(\mathbf{x}')\,\psi_\sigma^\dagger(\mathbf{x})\,\psi_\sigma(\mathbf{x})\,\psi_{\sigma'}(\mathbf{x}')\}$, respectively, where $\psi_\sigma(\mathbf{x})$ are operators corresponding to the particle spin components $\sigma=\uparrow,\downarrow$. Equation 3 is valid for both fermionic and bosonic statistics, under the approximations detailed above.

The current correlations comprise two terms: a pair correlation term proportional to $G_e^{(2)}(\mathbf{x}',\mathbf{x})$, giving rise to spatially and spectrally coherent spontaneous radiation (henceforth called coherent radiation) when substituted into Eq. 2, and a term proportional to the probability density $G_e^{(1)}(\mathbf{x},\mathbf{x})$, contributing a spatially and spectrally incoherent spontaneous radiation (*33*) (which we refer to as incoherent radiation). In this work, we focus on the case of a single particle, wherein $G_e^{(2)}(\mathbf{x}',\mathbf{x})=0$, and discuss the nature of quantum decoherence of the light it emits. A derivation of the effects of many-body quantum correlations [$G_e^{(2)}(\mathbf{x}',\mathbf{x})\neq 0$] on the radiation will be reported in a separate work (*53*).

Cherenkov radiation

CR is characterized by a directional, polarized, cone-shaped radiation pattern with opening semi-angle θ_c satisfying $\cos\theta_c=1/\beta n(\omega)$, where $\beta=v/c$ is the speed of the particles normalized by the speed of light and $n(\omega)$ is the refractive index of the medium. We assume that the emission is detected with a far-field detector located at a specific azimuthal angle on the cone's rim, providing broadband detection of all frequency components [note that in certain practical situations, the entire emission ring (over all azimuthal angles) could be collected using special optics (*54*)—thereby increasing the signal level]. Using the far-field expression for the dyadic Green tensor of a uniform dielectric medium (*52*), $\mathbf{G}(\mathbf{r},\mathbf{r}',\omega)=\frac{e^{ikr}}{4\pi r}(\mathbf{I}-\hat{\mathbf{r}}\hat{\mathbf{r}})\,e^{-i\mathbf{q}\cdot\mathbf{r}'}$, and assuming weak material dispersion, we find from Eqs. 2 and 3 that the radiation field projected on the detector is described by the following frequency-domain quantum autocorrelation (see section S3 for derivation)

$$\langle E^{(-)}(r,\omega')\,E^{(+)}(r,\omega)\rangle=\frac{U_0}{2\pi}\frac{e^{i(q_\omega-q_{\omega'})r}}{2n\epsilon_0cr^2}\int d^3\mathbf{x}\,e^{i(\mathbf{q}_\omega-\mathbf{q}_{\omega'})\cdot\mathbf{x}}G_e^{(1)}(\mathbf{x},\mathbf{x}) \quad (4)$$

where we denote $\mathbf{q}_\omega=\hat{\mathbf{r}}_c q_\omega$, with $\hat{\mathbf{r}}_c$ being the observation direction on the Cherenkov cone, $q_\omega=n(\omega)\omega/c$, and with $U_0=\hbar\omega\alpha\beta\sin^2\theta_c$. Equation 4 implies that for a single emitting particle, the first-order autocorrelation of CR is intimately related—through a Fourier transform—to the probability density of the particle wave function. The same conclusion—yet with more complex expressions—applies to all coherent CL processes, such as Smith-Purcell and transition radiation. Smith-Purcell radiation (*13*) occurs when an electron passes near a periodic grating. The grating introduces a boundary condition defining periodic photonic Bloch modes $\mathbf{u}_\kappa(\mathbf{r})$ (κ standing for all relevant indices such as Bloch vector, band number, and polarization). The periodicity of the photonic near field allows simultaneous energy and momentum conservation in the emission process, which results in the emission to the far field. A possible way to obtain the dyadic Green function of Eq. 2 is via mode expansion (*52*) $\mathbf{G}(\mathbf{r},\mathbf{r}',\omega)=\sum_\kappa c^2\mathbf{u}_\kappa(\mathbf{r})\,\mathbf{u}_\kappa^*(\mathbf{r}')/(\omega_\kappa^2-\omega^2)$, and a result similar to Eq. 4 could be derived.

Shock waves from quantum particles: Decoherence and a generalized uncertainty principle

The emission of classical shocks from a point charge (*9*), for which $\mathbf{j}(\mathbf{r},t)=e\mathbf{v}\delta(\mathbf{r}-\mathbf{v}t)$, is optically coherent over an arbitrarily wide spectral range only limited by the optical response of the medium. As such, the measured duration of the shock wave intensity envelope $|E(t)|^2$ is only limited by the material dispersion and/or the detection bandwidth, theoretically enabling shock waves on the

scale of femtoseconds and below (*8*, *9*). The quantum description, however, incorporates the finite-sized single-particle wave function through Eq. 4. The incoherent emission from different points on the wave function (resulting from the delta-function term in Eq. 3) is a manifestation of quantum decoherence of the emitted light, expected to inhibit interference visibility and stretch the shock duration. Here, the photon acts as the observed subsystem, and the electron it was emitted from acts as the unobserved subsystem (*47*). As these two subsystems are entangled in momentum and the electron degrees of freedom are now traced out, the different photon momenta tend to a classical mixture instead of a pure quantum superposition. As a result, the quantum coherence of that photon is hindered, and the interference visibility can be greatly reduced.

For CR, this observation manifests itself in a rather straightforward manner. Considering weakly dispersive media and wide detection bandwidths, the shock wave power envelope $P(t) = 2r^2\epsilon_0 nc\langle E^{(-)}(t)E^{(+)}(t)\rangle$ travelling at a group velocity v_g is given by the equal-time temporal Fourier transform of Eq. 4. The probability cloud $G_e^{(1)}(\mathbf{x},\mathbf{x})$ is projected along the direction of observation $\hat{\mathbf{r}}_c$ on the Cherenkov cone. From this relation, we find that if the emitting particle wave function has a momentum uncertainty Δp_e in the direction of CR, then the position uncertainty of the shock wave, Δx_{shw}, satisfies a generalized uncertainty principle (see section S3 for derivation)

$$\Delta x_{shw}\Delta p_e \geq \frac{\hbar}{2} \tag{5}$$

where the inequality becomes a strict equality for a minimum-uncertainty particle (satisfying $\Delta x_e \Delta p_e = \hbar/2$) and for broadband detection. The intuition behind Eq. 5 is the following: If the particle has a position uncertainty along the emission direction, the shock wave emitted from it will demonstrate this same position uncertainty. For a classical particle, this uncertainty approaches zero, giving a classical shock. However, for a quantum particle, the Heisenberg uncertainty principle (*55*) defines a lower bound to the position uncertainty, thereby affecting the presumably classical light.

The seemingly elementary result in Eq. 5 represents a rather deep conclusion: It demonstrates how the well-known classical wave interference can only be generated by a quantum particle that has a certain momentum uncertainty. This result also provides a fundamental quantum lower bound on the interference (the shock wave duration) that cannot be captured within a classical theory considering point particles or with a semiclassical theory treating the wave function as a coherent spread-out charge density (*33*, *41*) (see discussion below). As a concrete example, Fig. 2 shows how the momentum coherence $\delta p_e \leq \Delta p_e$ (or coherent momentum uncertainty) determines the tight lower bound on the shock duration. For example, particles in a mixed quantum state in momentum space, with low coherent uncertainty $\delta p_e \ll \Delta p_e$, emit temporally incoherent light and, consequently, a longer shock wave. These kinds of considerations also show why low-frequency radiation (radio frequency, microwave, etc.) will generally be classical.

Experimentally, the decoherence effect best manifests itself in the temporal (or spectral) autocorrelations $\langle E^{(-)}(t)E^{(+)}(t')\rangle$ [or $\langle E^{(-)}(\omega)E^{(+)}(\omega')\rangle$], where the off-diagonal ($t \neq t'$ or $\omega \neq \omega'$) terms relate to the coherence. Temporally coherent CR results in a transform-limited shock wave, as the classical theory suggests. However, the quantum corrections may alter the temporal behavior: Coherent (incoherent) shock waves exhibit $g^{(1)}(\tau)$ wider (narrower) than the pulse envelope. Figure 2 (C and D) demonstrates this behavior by simulating CR emission from 1-MeV electrons in silica for varying uncertainties. We note that this energy was chosen because it is closer to values often considered in high-energy physics to quantify Cherenkov detectors (with a relativistic particle velocity $\beta = 0.94$ close to 1), while being of a similar order of magnitude to what one finds in a transmission electron microscope (TEM). Lower electron energies (such as those useable in TEMs) could readily be considered, keeping in mind the experimental limitations detailed below in the "Experimental considerations" section.

In this context, it is noteworthy to mention that classical and semiclassical theories predict that the emitted radiation is always perfectly coherent, both temporally and spectrally. The reason for this lies in the treatment of the electron probability density $G_e^{(1)}(\mathbf{x},\mathbf{x})$ as a classical charge density that emits light coherently from different points. While this approximation holds in the limit of a point particle, it fails when the electron wave function is delocalized such that it exceeds the photon wavelength. Subsequently, it can be shown that these theories do not satisfy the quantum uncertainty principle (Eq. 5) in practical experimental situations of CR (e.g., in

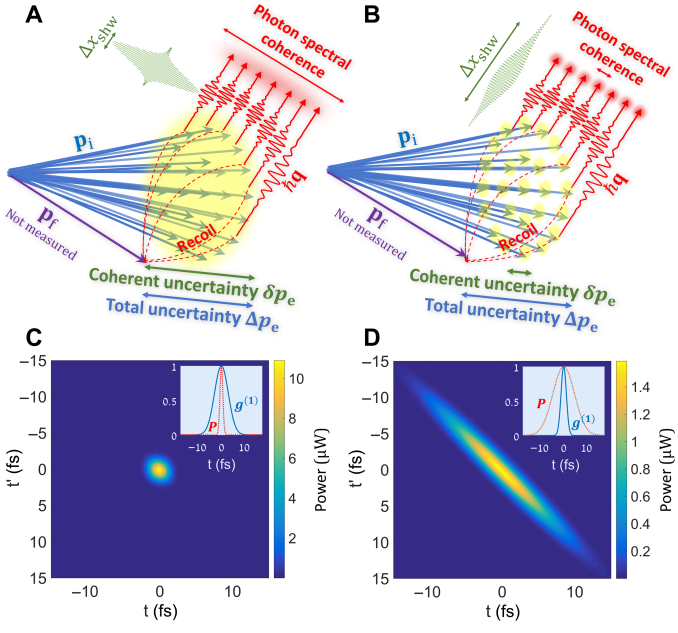

Fig. 2. How can particle momentum uncertainty determine the interference of waves emitted by that particle? (**A**) A quantum particle with a coherent momentum uncertainty δp_e that equals its total momentum uncertainty Δp_e displays a broad quantum coherence between its initial momenta $\mathbf{p}_i$ (yellow glow). When the particle transitions to any final momentum $\mathbf{p}_f$, the emitted wave inherits this initial coherence because of the "which path" interference between the initial particle states. Hence, different wave vector components of the wave are coherent (red glow). (**B**) A quantum particle in a mixture of momenta (total uncertainty Δp_e) with low coherent uncertainty $\delta p_e \ll \Delta p_e$ emits temporally incoherent waves. The limited interference inhibits the pulse formation, and its length exceeds the classical prediction. (**C** and **D**) The temporal field autocorrelations, $2r^2\epsilon_0 nc\langle E^{(-)}(t')E^{(+)}(t)\rangle$ (in μW), for 1-MeV electrons in silica in the visible range. The electrons are modeled as spherical Gaussian wave packets with coherent energy uncertainty (A) $\Delta\varepsilon_e = 3.72$ eV (wave packet radius ~50 nm) and (B) $\Delta\varepsilon_e = 0.19$ eV (wave packet radius ~1 μm). The diagonal ($t = t'$) indicates the temporal power envelope, $P(t)$, being transform-limited in (A) and incoherent in (B). Insets show a scaled comparison between $P(t)$ and the degree of first-order coherence of the light, $g^{(1)}(\tau)$. For both (A) and (B), the classically expected shock wave full width at half maximum is 1.4 fs.

standard electron microscopes)—as they always predict a larger optical coherence in the semiclassical picture (because quantum decoherence is ignored). One is able to amend the semiclassical picture by adopting an ad hoc probabilistic approach (*33*) demanding that the electron emits light incoherently from different points, although a fully quantum treatment is necessary to unveil other important aspects such as quantum correlations (*53*, *56*). An elaborate comparison between these theories can be found in section S7 and other works (*32*, *33*, *41*).

Measuring the particle wave function dimensions using Cherenkov detectors

Quantum optical measurement of the spectral autocorrelations may unveil information about the emitter wave function itself and provide an unprecedented analytical tool for particle identification. Equation 4 provides a direct relation between the frequency-domain autocorrelation $\langle E^{(-)}(\omega')E^{(+)}(\omega)\rangle$ and the spatial Fourier transform (or structure factor) of the emitter probability density $G_e^{(1)}(\mathbf{x},\mathbf{x})$. This structure factor is equivalent to a momentum coherence function of the particle $\varrho_e(\mathbf{q}_\omega - \mathbf{q}_{\omega'}) = \int d^3\mathbf{k}\, \rho_e(\mathbf{k}+\mathbf{q}_{\omega'}, \mathbf{k}+\mathbf{q}_\omega)$, namely

$$\langle E^{(-)}(\omega')\, E^{(+)}(\omega)\rangle \propto \int d^3\mathbf{x}\, e^{i(\mathbf{q}_\omega - \mathbf{q}_{\omega'})\cdot\mathbf{x}} G_e^{(1)}(\mathbf{x},\mathbf{x}) = \varrho_e(\mathbf{q}_\omega - \mathbf{q}_{\omega'}) \quad (6)$$

Equation 6 implies that a spontaneously emitted photon is only as spectrally coherent as the emitting particle it originated from (see Fig. 2, A and B). Spontaneous CR can, therefore, be used to map the structure of the emitter wave function and its momentum coherence by analyzing the correlations of emitted photons. Note that only the spectral coherence of the photons plays a role here, namely, the width of the off-diagonal part of the autocorrelations (see Fig. 3C). The diagonal part (optical power spectrum), $\langle E^{(-)}(\omega)E^{(+)}(\omega)\rangle$, is wave function independent.

The wave function size and shape can be estimated, for example, by assuming a spatial variance matrix for the emitter probability cloud given as $\mathbf{\Delta}_{ij}^2 = \mathrm{Tr}\{\mathbf{r}_i\mathbf{r}_j\boldsymbol{\rho}_e\}$. The photons are collected at an observation direction $\hat{\mathbf{r}}_c$ on the Cherenkov cone, and the width of their spectral coherence $\Delta\omega$ is measured (see Fig. 3, A to C). It then gives an estimate for the wave function dimensions $\mathbf{\Delta}$ along the observation direction (see section S4 for the derivation)

$$\hat{\mathbf{r}}_c^T \mathbf{\Delta}^2 \hat{\mathbf{r}}_c = \frac{v_g^2}{\Delta\omega^2} \quad (7)$$

where v_g denotes the shock wave group velocity. If the electron wave function is not spherical, we can further reconstruct the three-dimensional $\mathbf{\Delta}$ by measuring the spectral coherence along different Cherenkov cones $\hat{\mathbf{r}}_c$ [which can be done by measurements of multiple particles with the same wave function moving through media of different refractive indices n, as done in threshold detection (*16*)]. At least two such measurements are necessary to find both the longitudinal and transverse sizes of the wave function.

The quantum optical measurements necessary for the reconstruction of the photon density matrix in the frequency domain have been demonstrated experimentally for single photons (*57*–*59*). Combining these quantum optical reconstruction techniques with Cherenkov detectors may allow for completely new and exciting capabilities. Currently available techniques for particle identification in Cherenkov detectors are limited to measuring velocity or mass (*16*, *17*). Our proposed scheme further enables the measurement of the wave function dimensions and coherences of naturally occurring particles such as in cosmic radiation and beta decay (*16*), as well as the characterization of charged particle beams (for example in microscopy). Figure 3 (D and E) shows an example for such measurement scheme for the case of 1-MeV electrons. This method can provide an alternative to matter wave holography [used in electron microscopes (*60*) to measure the transverse wave function], which is currently unavailable for high-energy charged particles, such as muons, protons, kaons, and pions. In contrast, the measurement we propose is relevant for these particles and can be used as part of Cherenkov detectors, which also have the advantage of being a nondestructive measurement.

Beyond the capability of reconstructing the wave function size, our technique can be used to detect the signature of non-Gaussian wave packets (in energy-time space), such as coherent electron

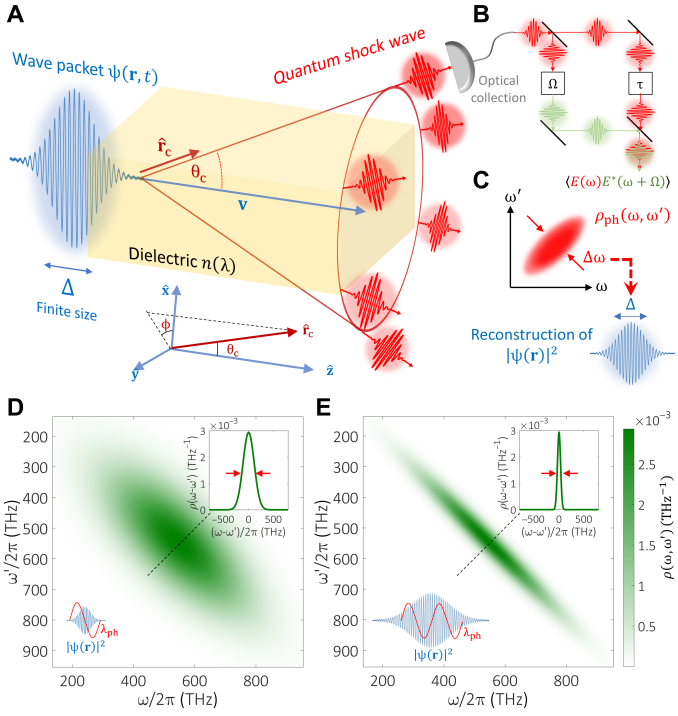

Fig. 3. Quantum optical analysis of CR—for measuring the emitter's wave function. (**A**) A charged particle wave packet $\psi(\mathbf{r}, t)$ of finite size Δ and carrier velocity $\mathbf{v_0}$ impinges on a Cherenkov detector with material dispersion $n(\omega)$. The particle spontaneously emits quantum shock waves of light into a cone with opening half-angle $\theta_c(\omega) = \mathrm{acos}[1/\beta n(\omega)]$. Collection optics is situated along the cone in the direction $\hat{\mathbf{r}}_c$ in the far field. (**B**) Detection scheme for measuring the spectral field autocorrelations $\langle E(\omega)E(\omega')\rangle$ using an interference between spectrally/temporally sheared fields (*57*). (**C**) The reconstructed photon density matrix determines the spatial probability distribution $|\psi(\mathbf{r})|^2$. (**D** and **E**) Simulation of particle wave function size reconstruction from the photon density matrix. A single 1-MeV electron ($\beta = 0.94$) in a silica Cherenkov detector [dispersion taken from (*77*)] emits CR that is collected within the visible range ($\lambda = 400$ to 700 nm, centered at $\lambda_0 = 550$ nm). The electron wave function envelope is Gaussian and spherically symmetric, with position uncertainty of (*d*) $\Delta x_e = 254$ nm and (E) $\Delta x_e = 1016$ nm (bottom insets). In both (D) and (E), the measured photon density matrix, $\rho_{ph}(\omega, \omega')$, is plotted. The wave function–independent diagonal $\rho_{ph}(\omega, \omega)$ that denotes the photodetection probability is the same for both cases. However, the off-diagonal spectral coherence $\rho_{ph}(\omega - \omega')$ is strongly dependent on the wave function. Measuring its width $\Delta\omega_{coh}$ (top insets) and using the approximate Eq. 7 provide the estimates (D) $\Delta\tilde{x}_e = 290$ nm and (E) $\Delta\tilde{x}_e = 1006$ nm.

energy combs produced in photon-induced near-field electron microscopy (PINEM) (*61*), ultrafast TEM (*27*), and other methods (see Fig. 4) (*62*–*64*). In PINEM, a free electron traverses a near-field optical structure and interacts with a coincident laser pulse. As a result, the electron wave function is modulated and given by a coherent superposition of energy levels. Following free-space propagation, the electron wave function takes the form of a pulse train (*27*). When this electron emits CR, notice how the interference fringes due to its shaped wave function appear only in the photon spectral autocorrelations (off-diagonal) and not in the radiation spectrum (diagonal).

Experimental considerations

Here, we briefly discuss some important considerations for realizing our predictions in an experiment. For the analysis discussed in the previous section, the electron's coherent interaction length L_{int} must be in the range $\lambda/n \ll L_{\mathrm{int}} \ll (n/\Delta n)(\lambda/\Delta\lambda)\beta\lambda$, where $\Delta n = n - n_g$ is the difference between the refractive and group indices of the material, and $\Delta\lambda$ denotes the wavelength band collected by the detection system (see section S5). The lower limit ensures that the Cherenkov angle is sharply defined, while the upper limit ensures that the material dispersion has a weak effect on the correlation between different frequencies. For standard materials and optical wavelengths, L_{int} is in the order of a few micrometers.

For CR in bulk media, other scattering processes with mean free paths smaller than L_{int} can readily broaden the particle spectrum $\rho_e(\mathbf{k}, \mathbf{k})$. In section S6, we show that for a general uniform medium of optical response function Im $\mathbf{G}(\mathbf{q}, \omega)$ (which encompasses all types of inelastic processes, such as scattering by phonons and plasmons, and excitations of electron-hole pairs), the momentum coherence function $\varrho_e(\mathbf{q}_\omega - \mathbf{q}_{\omega'})$ of Eq. 6 remains unchanged. As the latter quantity is the one responsible for the Cherenkov autocorrelation through Eq. 6, we expect the signature of the wave function to persist. In electron microscopy, one can avoid these scattering processes by using an aloof beam geometry having electrons that propagate in vacuum near an optical structure, such as in Smith-Purcell experiments or in emission of Cherenkov photons near dielectric boundaries (*65*).

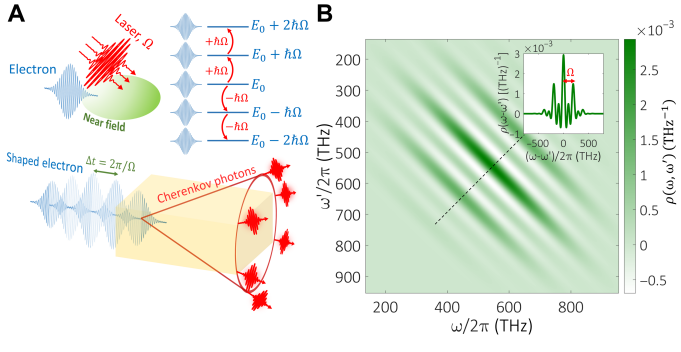

Fig. 4. Quantum optical analysis of CR—emitted from a laser-driven electron wave function. (**A**) A free electron wave function is shaped by the interaction with a strong laser field of frequency Ω (here, $\Omega = 2\pi \times 200$ THz), as done in photon-induced near-field electron microscopy (*61*). The result is a coherent electron energy ladder, manifested as a temporal pulse train. (**B**) Cherenkov photon autocorrelations reveal the electron wave function spectral interference pattern, matching the laser frequency. The measurement scheme is the same as in Fig. 3 (A to C).

DISCUSSION

Here, we investigated light emission by free charged particles from a quantum-optical viewpoint, by using a fully quantum formalism of light-matter interaction. Our conclusions take into account the experimental situation that the emitting particle itself is not measured. In this situation, recent studies show that the particle wave function has no influence on the emitted spectrum. We complement this realization by showing that quantum optical observables such as the emitted pulse duration and optical autocorrelations are all strongly influenced by the particle wave function. Moreover, all the quantum features of the particle such as coherence, uncertainty, and correlations embedded in the emitter wave function play an important role in determining the properties of the emitted light.

As an example, we considered the Cherenkov effect, and its characteristic optical shock wave, envisioned classically for almost a century as a coherent, transform-limited pulse of light. Instead, we found that it is fundamentally limited by the particle quantum uncertainty, satisfying a generalized uncertainty principle. The smaller the coherent momentum uncertainty of the particle is, the longer (and less coherent) the shock wave becomes. We further showed how this uncertainty relation can be harnessed to unveil information about the particle wave function, allowing unprecedented capabilities for particle detection. For example, Cherenkov detectors together with a quantum-optical measurement of the emitted light can be used to reconstruct the particle wave function size, shape, coherence, and quantum correlations.

Our findings can be used to resolve an important fundamental question of practical importance: What part of the energy uncertainty of a free electron is coherent, and what part is incoherent? This property can be measured from the radiation autocorrelations and spectrum. With the advent of laser-driven electron sources, for example, in ultrafast electron microscopes (*25*–*27*, *63*, *66*, *67*), the particle coherent energy uncertainty is believed to be dictated by the laser linewidth (*26*, *68*), e.g., spanning tens of millielectron volts for excitations with femtosecond lasers. With the ability to coherently control the spatial electron wave function (*23*, *24*), the transverse momentum uncertainty can be further lowered. Such conditions allow for the predictions of our work to be tested experimentally under controllable settings.

Considering the outlook for using free electrons as quantum probes (*15*, *51*, *69*), our work paves the way toward quantum measurement of free electrons and other charged particles based on spontaneous emission. One interesting direction for extending the research is to consider light emission from low-energy (tens to hundreds of electron volts) coherent electrons (*70*, *71*), for which the zero-recoil approximation is no longer valid. In addition to recoil-induced quantum corrections in the emitted light (*45*), we expect the coherence of such light to be limited by the high spatial coherence of the electrons. Furthermore, our results may readily be generalized to other physical mechanisms of wave emission, for example, analogs of the Cherenkov effect (*72*, *73*), as in Bose-Einstein condensates. Similar effects can be explored with any photonic quasiparticle (*74*), and even with sound waves, and phonon waves in solids (*75*), which all have the same underlying quantum nature and must have exact analogous phenomena.

Another intriguing question is the effect of many-body correlations (as manifested by the second term in Eq. 2) on such radiation phenomena, giving rise to yet unexplored quantum super- and subradiance regimes of coherent CL. These arise from coherent interference of

multiparticle wave functions, which will be discussed in forthcoming work (*53*).

Note added in proof: This work was first presented in the Conference on Lasers and Electro-Optics in May 2020 as a conference presentation (*76*). A related paper (doi: 10.1126/sciadv.abf6380) appears in *Science Advances*.

SUPPLEMENTARY MATERIALS

Supplementary material for this article is available at http://advances.sciencemag.org/cgi/content/full/7/18/eabf8096/DC1

REFERENCES AND NOTES

1. J. D. Jackson, *Classical Electrodynamics* (Wiley, 1999).
2. L. E. Kinsler, *Fundamentals of Acoustics* (Wiley, ed. 4, 2000).
3. B. Méhauté, *An Introduction to Hydrodynamics and Water Waves* (Springer Berlin Heidelberg, 1976).
4. P. A. Cherenkov, Visible emission of clean liquids by action of γ radiation. *Dokl. Akad. Nauk SSSR* **2**, 451 (1934).
5. J. V. Jelley, B. M. Bolotovski, E. M. Lekin, Cerenkov radiation and its applications. *J. Appl. Phys.* **6**, 227 (1955).
6. I. Frank, I. Tamm, Coherent visible radiation of fast electrons passing through matter, in *Selected Papers* (Springer Berlin Heidelberg, 1991), vol. 93, pp. 29–35.
7. A. A. Watson, The discovery of Cherenkov radiation and its use in the detection of extensive air showers. *Nucl. Phys. B Proc. Suppl.* **212–213**, 13–19 (2011).
8. B. J. M. Brenny, A. Polman, F. J. García de Abajo, Femtosecond plasmon and photon wave packets excited by a high-energy electron on a metal or dielectric surface. *Phys. Rev. B* **94**, 155412 (2016).
9. G. N. Afanasiev, *Vavilov-Cherenkov and Synchrotron Radiation: Foundations and Applications* (Kluwer Academic Publishers, 2005).
10. F. J. García de Abajo, Optical excitations in electron microscopy. *Rev. Mod. Phys.* **82**, 209–275 (2010).
11. A. Friedman, A. Gover, G. Kurizki, S. Ruschin, A. Yariv, Spontaneous and stimulated emission from quasifree electrons. *Rev. Mod. Phys.* **60**, 471–535 (1988).
12. I. M. Frank, V. L. Ginzburg, Radiation of a uniform moving electron due to its transition from one medium into another. *J. Phys.* **9**, 353–362 (1945).
13. S. J. Smith, E. M. Purcell, Visible light from localized surface charges moving across a grating. *Phys. Rev.* **92**, 1069–1069 (1953).
14. H. Motz, W. Thon, R. N. Whitehurst, Experiments on radiation by fast electron beams. *J. Appl. Phys.* **24**, 826–833 (1953).
15. A. Polman, M. Kociak, F. J. García de Abajo, Electron-beam spectroscopy for nanophotonics. *Nat. Mater.* **18**, 1158–1171 (2019).
16. L. Cerrito, *Radiation and Detectors: Introduction to the Physics of Radiation and Detection Devices* (Springer, 2017).
17. T. Ypsilantis, J. Seguinot, Theory of ring imaging Cherenkov counters. *Nucl. Inst. Methods Phys. Res. A* **343**, 30–51 (1994).
18. B. W. J. Mcneil, N. R. Thompson, X-ray free-electron lasers. *Nat. Photonics* **4**, 814–821 (2010).
19. A. Massuda, C. Roques-Carmes, Y. Yang, S. E. Kooi, Y. Yang, C. Murdia, K. K. Berggren, I. Kaminer, M. Soljačić, Smith-Purcell radiation from low-energy electrons. *ACS Photonics* **5**, 3513–3518 (2018).
20. G. Adamo, K. F. MacDonald, Y. H. Fu, C. M. Wang, D. P. Tsai, F. J. García de Abajo, N. I. Zheludev, Light well: A tunable free-electron light source on a chip. *Phys. Rev. Lett.* **103**, 113901 (2009).
21. E. Ciarrocchi, N. Belcari, Cerenkov luminescence imaging: Physics principles and potential applications in biomedical sciences. *EJNMMI Physics* **4**, 14 (2017).
22. A. M. Cook, R. Tikhoplav, S. Y. Tochitsky, G. Travish, O. B. Williams, J. B. Rosenzweig, Observation of narrow-band terahertz coherent cherenkov radiation from a cylindrical dielectric-lined waveguide. *Phys. Rev. Lett.* **103**, 095003 (2009).
23. R. Shiloh, Y. Lereah, Y. Lilach, A. Arie, Sculpturing the electron wave function using nanoscale phase masks. *Ultramicroscopy* **144**, 26–31 (2014).
24. J. Verbeeck, H. Tian, P. Schattschneider, Production and application of electron vortex beams. *Nature* **467**, 301–304 (2010).
25. A. Feist, K. E. Echternkamp, J. Schauss, S. V. Yalunin, S. Schäfer, C. Ropers, Quantum coherent optical phase modulation in an ultrafast transmission electron microscope. *Nature* **521**, 200–203 (2015).
26. G. M. Vanacore, I. Madan, G. Berruto, K. Wang, E. Pomarico, R. J. Lamb, D. McGrouther, I. Kaminer, B. Barwick, F. J. García de Abajo, F. Carbone, Attosecond coherent control of free-electron wave functions using semi-infinite light fields. *Nat. Commun.* **9**, 2694 (2018).
27. K. E. Priebe, C. Rathje, S. V. Yalunin, T. Hohage, A. Feist, S. Schäfer, C. Ropers, Attosecond electron pulse trains and quantum state reconstruction in ultrafast transmission electron microscopy. *Nat. Photonics* **11**, 793–797 (2017).
28. C. Mechel, Y. Kurman, A. Karnieli, N. Rivera, A. Arie, I. Kaminer, Imaging the collapse of electron wave-functions: the relation to plasmonic losses, in *Conference on Lasers and Electro-Optics FF3M.6* (OSA, 2019).
29. O. Kfir, Entanglements of electrons and cavity photons in the strong-coupling regime. *Phys. Rev. Lett.* **123**, 103602 (2019).
30. G. Guzzinati, A. Béché, H. Lourenço-Martins, J. Martin, M. Kociak, J. Verbeeck, Probing the symmetry of the potential of localized surface plasmon resonances with phase-shaped electron beams. *Nat. Commun.* **8**, 14999 (2017).
31. I. P. Ivanov, V. G. Serbo, V. A. Zaytsev, Quantum calculation of the Vavilov-Cherenkov radiation by twisted electrons. *Phys. Rev. A* **93**, 53825 (2016).
32. Y. Pan, A. Gover, Spontaneous and stimulated emissions of a preformed quantum free-electron wave function. *Phys. Rev. A* **99**, 052107 (2019).
33. R. Remez, A. Karnieli, S. Trajtenberg-Mills, N. Shapira, I. Kaminer, Y. Lereah, A. Arie, Observing the quantum wave nature of free electrons through spontaneous emission. *Phys. Rev. Lett.* **123**, 060401 (2019).
34. Y. Pan, A. Gover, Spontaneous and stimulated radiative emission of modulated free-electron quantum wavepackets—Semiclassical analysis. *J. Phys. Commun.* **2**, 115026 (2018).
35. C. Luo, M. Ibanescu, S. G. Johnson, J. D. Joannopoulos, Cerenkov radiation in photonic crystals. *Science* **299**, 368–371 (2003).
36. Z. Wang, K. Yao, M. Chen, H. Chen, Y. Liu, Manipulating Smith-Purcell emission with babinet metasurfaces. *Phys. Rev. Lett.* **117**, 157401 (2016).
37. L. Liang, W. Liu, Y. Liu, Q. Jia, L. Wang, Y. Lu, Multi-color and multidirectional-steerable Smith-Purcell radiation from 2D sub-wavelength hole arrays. *Appl. Phys. Lett.* **113**, 013501 (2018).
38. S. Liu, M. Hu, Y. Zhang, Y. Li, R. Zhong, Electromagnetic diffraction radiation of a subwavelength-hole array excited by an electron beam. *Phys. Rev. E* **80**, 036602 (2009).
39. A. Gover, R. Ianconescu, A. Friedman, C. Emma, N. Sudar, P. Musumeci, C. Pellegrini, Superradiant and stimulated-superradiant emission of bunched electron beams. *Rev. Mod. Phys.* **91**, 035003 (2019).
40. N. Talebi, Schrödinger electrons interacting with optical gratings: Quantum mechanical study of the inverse Smith–Purcell effect. *New J. Phys.* **18**, 123006 (2016).
41. A. Gover, Y. Pan, Dimension-dependent stimulated radiative interaction of a single electron quantum wavepacket. *Phys. Lett. A* **382**, 1550–1555 (2018).
42. With the only exception being in case the final state is post-selected; see reference number 30. *Nat. Commun.* 8, 14999 (2017).
43. V. L. Ginzburg, Quantum theory of radiation of electron uniformly moving in medium. *Zh. Eksp. Teor. Fiz.* **10**, 589–600 (1940).
44. I. Kaminer, M. Mutzafi, A. Levy, G. Harari, H. Herzig Sheinfux, S. Skirlo, J. Nemirovsky, J. D. Joannopoulos, M. Segev, M. Soljačić, Quantum Čerenkov radiation: Spectral cutoffs and the role of spin and orbital angular momentum. *Phys. Rev. X* **6**, 011006 (2016).
45. S. Tsesses, G. Bartal, I. Kaminer, Light generation via quantum interaction of electrons with periodic nanostructures. *Phys. Rev. A* **95**, 013832 (2017).
46. M. O. Scully, O. Marlan, M. S. Zubairy, *Quantum optics* (Cambridge Univ. Press, 1997).
47. E. Joos, H. D. Zeh, C. Kiefer, D. Giulini, J. Kupsch, I. O. Stamatescu, *Decoherence and the Appearance of a Classical World in Quantum Theory* (Springer Berlin Heidelberg, 2003).
48. B. E. A. Saleh, M. C. Teich, *Fundamentals of Photonics* (Wiley-Interscience, 2007).
49. N. Bohr, J. R. Nielsen, *The Correspondence Principle: 1918–1923* (North-Holland Pub. Co., 1976).
50. Z. Zhao, X.-Q. Sun, S. Fan, Quantum entanglement and modulation enhancement of free-electron-bound-electron interaction. *arXiv* 2010.11396, (2020).
51. A. Gover, A. Yariv, Free-electron-bound-electron resonant interaction. *Phys. Rev. Lett.* **124**, 064801 (2020).
52. L. Novotny, B. Hecht, *Principles of Nano-optics. Principles of Nano-Optics* (Cambridge Univ. Press, 2006).
53. A. Karnieli, N. Rivera, A. Arie, I. Kaminer, Super- and subradiance by entangled free particles. https://arxiv.org/abs/2011.02548 (2020).
54. K. Nanbu, Y. Saito, H. Saito, S. Kashiwagi, F. Hinode, T. Muto, H. Hama, Bunch length measurement employing cherenkov radiation from a thin silica aerogel. *Particles* **1**, 305–314 (2018).
55. J. J. Sakurai, J. Napolitano, *Modern Quantum Mechanics* (Addison-Wesley, 2011).
56. C. Mechel, Y. Kurman, A. Karnieli, N. Rivera, A. Arie, I. Kaminer, Quantum correlations in electron microscopy. *Optica* **8**, 70–78 (2021).
57. A. O. C. Davis, V. Thiel, M. Karpiński, B. J. Smith, Measuring the single-photon temporal-spectral wave function. *Phys. Rev. Lett.* **121**, 083602 (2018).
58. W. Wasilewski, P. Kolenderski, R. Frankowski, Spectral density matrix of a single photon measured. *Phys. Rev. Lett.* **99**, 123601 (2007).

59. A. O. C. Davis, V. Thiel, M. K. Karpínski, B. J. Smith, Experimental single-photon pulse characterization by electro-optic shearing interferometry. *Phys. Rev. A* **98**, 23840 (2018).
60. H. Lichte, M. Lehmann, Electron holography—Basics and applications. *Reports Prog. Phys.* **71**, 016102 (2008).
61. B. Barwick, D. J. Flannigan, A. H. Zewail, Photon-induced near-field electron microscopy. *Nature* **462**, 902–906 (2009).
62. D. S. Black, U. Niedermayer, Y. Miao, Z. Zhao, O. Solgaard, R. L. Byer, K. J. Leedle, Net acceleration and direct measurement of attosecond electron pulses in a silicon dielectric laser accelerator. *Phys. Rev. Lett.* **123**, 264802 (2019).
63. Y. Morimoto, P. Baum, Diffraction and microscopy with attosecond electron pulse trains. *Nat. Phys.* **14**, 252–256 (2018).
64. M. Kozák, N. Schönenberger, P. Hommelhoff, Ponderomotive generation and detection of attosecond free-electron pulse trains. *Phys. Rev. Lett.* **120**, 103203 (2018).
65. R. Dahan, S. Nehemia, M. Shentcis, O. Reinhardt, Y. Adiv, X. Shi, O. Be'er, M. H. Lynch, Y. Kurman, K. Wang, I. Kaminer, Resonant phase-matching between a light wave and a free-electron wavefunction. *Nat. Phys.* **16**, 1123–1131 (2020).
66. K. Wang, R. Dahan, M. Shentcis, Y. Kauffmann, A. Ben Hayun, O. Reinhardt, S. Tsesses, I. Kaminer, Coherent interaction between free electrons and a photonic cavity. *Nature* **582**, 50–54 (2020).
67. O. Kfir, H. Lourenço-Martins, G. Storeck, M. Sivis, T. R. Harvey, T. J. Kippenberg, A. Feist, C. Ropers, Controlling free electrons with optical whispering-gallery modes. *Nature* **582**, 46–49 (2020).
68. E. Pomarico, I. Madan, G. Berruto, G. M. Vanacore, K. Wang, I. Kaminer, F. J. García de Abajo, F. Carbone, meV resolution in laser-assisted energy-filtered transmission electron microscopy. *ACS Photonics* **5**, 759–764 (2018).
69. A. Gover, B. Zhang, D. Ru, R. Ianconescu, A. Friedman, J. Scheuer, A. Yariv, Resonant interaction of modulation-correlated quantum electron wavepackets with bound electron states. *arXiv* 2010.15756, (2020).
70. J. N. Longchamp, T. Latychevskaia, C. Escher, H. W. Fink, Graphene unit cell imaging by holographic coherent diffraction. *Phys. Rev. Lett.* **110**, 255501 (2013).
71. S. Meier, T. Higuchi, M. Nutz, A. Högele, P. Hommelhoff, High spatial coherence in multiphoton-photoemitted electron beams. *Appl. Phys. Lett.* **113**, 143101 (2018).
72. I. Carusotto, S. X. Hu, L. A. Collins, A. Smerzi, Bogoliubov-Čerenkov radiation in a Bose-Einstein condensate flowing against an obstacle. *Phys. Rev. Lett.* **97**, (2006).
73. P. Genevet, D. Wintz, A. Ambrosio, A. She, R. Blanchard, F. Capasso, Controlled steering of Cherenkov surface plasmon wakes with a one-dimensional metamaterial. *Nat. Nanotechnol.* **10**, 804–809 (2015).
74. N. Rivera, I. Kaminer, Light–matter interactions with photonic quasiparticles. *Nat. Rev. Phys.* **2**, 538–561 (2020).
75. T. I. Andersen, B. L. Dwyer, J. D. Sanchez-Yamagishi, J. F. Rodriguez-Nieva, K. Agarwal, K. Watanabe, T. Taniguchi, E. A. Demler, P. Kim, H. Park, M. D. Lukin, Electron-phonon instability in graphene revealed by global and local noise probes. *Science* **364**, 154–157 (2019).
76. A. Karnieli, N. Rivera, A. Arie, I. Kaminer, Unveiling emitter wavefunction size via the quantum coherence of its radiation, in *Conference on Lasers and Electro-Optics* (CLEO, 2020).
77. I. Malitson, H. Interspecimen, Interspecimen comparison of the refractive index of fused silica. *J. Opt. Soc. Am.* **55**, 1205 (1965).
78. E. G. Harris, *A Pedestrian Approach to Quantum Field Theory* (Dover Publications, 2014).
79. J. C. Garrison, R. Y. Chiao, *Quantum Optics* (Oxford Univ. Press, 2008).

Acknowledgments

Funding: This work was supported by the ERC starting grant NanoEP 851780 and the Israel Science Foundation grants 3334/19, 831/19, and 1415/17. A.K. acknowledges support by the Adams Fellowship of the Israeli Academy of Sciences and Humanities. N.R. was supported by the Department of Energy Fellowship DE-FG02-97ER25308 and by a Dean's Fellowship by the MIT School of Science. **Author contributions:** A.K., N.R., A.A., and I.K. conceived the idea and contributed to writing the paper. A.K. performed the theoretical derivations. **Competing interests:** The authors declare that they have no competing interests. **Data and materials availability:** All data needed to evaluate the conclusions in the paper are present in the paper and/or the Supplementary Materials. Additional data related to this paper may be requested from the authors.

Submitted 20 November 2020
Accepted 19 March 2021
Published 30 April 2021
10.1126/sciadv.abf8096

Citation: A. Karnieli, N. Rivera, A. Arie, I. Kaminer, The coherence of light is fundamentally tied to the quantum coherence of the emitting particle. *Sci. Adv.* **7**, eabf8096 (2021).

The coherence of light is fundamentally tied to the quantum coherence of the emitting particle

Aviv Karnieli, Nicholas Rivera, Ady Arie and Ido Kaminer

Sci Adv **7** (18), eabf8096.
DOI: 10.1126/sciadv.abf8096